

Design and Motion Control of a 2-DoF Exoskeleton Robot for Ankle Joint Rehabilitation of Post-Stroke Patients

Eko Wahyu Abryandoko

Industrial Engineering Department, University of Bojonegoro, Indonesia
abryandoko@gmail.com (corresponding author)

Faisal Ashari

Industrial Engineering Department, University of Bojonegoro, Indonesia
faisal.gaxes@gmail.com

Received: 6 May 2025 | Revised: 21 June 2025 | Accepted: 3 July 2025

Licensed under a CC-BY 4.0 license | Copyright (c) by the authors | DOI: <https://doi.org/10.48084/etasr.11943>

ABSTRACT

Post-stroke patients often experience motor function impairments in the lower extremities, including the ankle joint, which can hinder walking ability and body balance. Rehabilitation plays a crucial role in restoring these functions; however, it typically requires a lengthy process and intensive involvement from medical professionals. This study aims to design and develop a Two-Degree-of-Freedom (2-DoF) ankle exoskeleton system, incorporating dorsiflexion–plantarflexion and inversion–eversion movements, as an alternative automated and programmable rehabilitation therapy. The system's performance was evaluated by comparing the actual joint movement angles with reference angles set through preset inputs. Tests were conducted under both unloaded conditions and loaded conditions simulating the limb mass of users. The results showed that for dorsiflexion–plantarflexion movements, the average angle error was 1.9° under unloaded conditions, increasing to 2.7° when a load was applied. For inversion–eversion movements, the average error was 2.4° without load and 3.2° with load. The system demonstrated operational stability and consistency in following the programmed motion trajectories. Based on these findings, the developed exoskeleton has potential as an effective, safe, and efficient rehabilitation therapy device to support functional recovery in post-stroke patients.

Keywords- exoskeleton; post-stroke rehabilitation; ankle joint; angle tracking

I. INTRODUCTION

Stroke is one of the leading causes of long-term disability worldwide, with more than 4 million cases reported annually [1, 2]. The majority of stroke patients experience motor function impairments, particularly in the lower extremities, resulting in reduced walking ability, compromised balance, and limitations in performing daily activities independently. Approximately 65% of patients require ongoing rehabilitation programs to restore their motor functions [3]. However, conventional rehabilitation methods that rely on manual therapy from medical professionals have several limitations. According to authors in [4], an imbalance between the number of patients and available therapists, high workloads, and inconsistencies in exercise intensity and duration contribute to suboptimal recovery outcomes. These challenges are further compounded by the financial burden placed on patients undergoing long-term therapy [5]. Technological advancements have opened new opportunities in the field of rehabilitation, particularly through the use of robotic devices

such as exoskeletons to assist lower limb movements in both passive and active training modes [6-8].

The presence of exoskeletons can increase the intensity, consistency, and efficiency of exercise, as well as accelerate the recovery of motor function through neuroplasticity stimulation [9]. Several recent studies have developed a Two-Degree-of-Freedom (2-DoF) ankle exoskeleton design mechanism using pneumatic actuators [10], or a bidirectional tendon cable drive mechanism utilizing adaptive control of PID neural networks [11]. Although both of these approaches offer high precision, their design and control systems are much more complex, requiring additional infrastructure such as air compressors and complex nonlinear controls. This condition makes it difficult to apply them in self-therapy, especially in household environments or facilities with limited resources. In addition, most advanced exoskeleton systems use Electromyography (EMG) and Electroencephalography (EEG) sensors to detect patient movement intentions and perform adaptive control based on admittance or impedance [12, 13]. Although this approach is effective, such systems have limitations in terms of complexity, cost, and the need for

routine calibration and technical knowledge from the user [14]. The design of exoskeletons based on mechanical control without relying on biological signals can be a relevant option to support these needs. Control systems, such as admittance [15] and impedance [16], have been widely applied in lower limb exoskeleton systems due to their ability to adapt motor movements to the interaction forces between humans and robots. This approach allows the system to automatically direct the motors in the direction that minimizes the interaction forces, thus creating flexible and adaptive movements during the therapy process [17]. However, the physical interaction between the user and the exoskeleton is dynamic throughout the exercise, so the controller must be able to adjust parameters in real-time based on the user's biomechanical conditions.

This research proposes a 2-DoF ankle exoskeleton design with simple mechanical control using servo motors and preset angle inputs. This approach does not require biological signals or complex adaptive control, yet it can still provide accurate and stable motion tracking. Its lightweight, easy-to-operate structure makes the exoskeleton a promising solution for independent post-stroke rehabilitation. The control strategy uses a feedforward torque calculation and a PID control loop with angle feedback from an encoder sensor, enabling real-time correction of deviations for smooth motion and ensuring user safety and comfort during rehabilitation. The 2-DoF ankle exoskeleton design focuses on dorsiflexion–plantarflexion and inversion–eversion movements for post-stroke patient rehabilitation applications. The system uses servo motors as the main actuators, controlled by a microcontroller. A motion angle tracking test was conducted to verify the conformity of the movement with the patient's physiological limits. The main objectives of this study include: (1) designing the mechanical structure of the exoskeleton to be able to follow the natural movement of the ankle, (2) developing a microcontroller-based control system with preset angle reference inputs, (3) implementing the actual angle tracking system to validate movement accuracy, and (4) evaluating system performance through functional tests on the effects of user load variations. The expected end result is a safe, programmed rehabilitation system that can increase the effectiveness of patient motor recovery.

II. DESIGN AND SYSTEM ARCHITECTURE OF THE EXOSKELETON

The mechanical design of the exoskeleton is intended to support ankle joint rehabilitation through two primary movements: dorsiflexion–plantarflexion and inversion–eversion. The system adopts a 2-DoF configuration to accurately replicate the physiological movements of the human ankle.

A. Robot Principles

Ankle movement is a complex biomechanical system, with the ankle joint playing a critical role in maintaining stability during walking. The development of the exoskeleton design in this study focuses on ankle rehabilitation, specifically to facilitate two main movements: dorsiflexion–plantarflexion and inversion–eversion. The biomechanical system of the human ankle serves as the foundation for the exoskeleton design. This

joint is a complex articulation between the tibia, fibula, and talus bones, which allows various movements such as plantarflexion (foot-down movement), dorsiflexion (toe-up movement), and limited rotational movements such as inversion, eversion, pronation, and supination [18, 19]. Anatomical variations between individuals, as well as cultural and geographic factors, can affect the natural range of ankle motion. Therefore, the exoskeleton control system is designed to be flexible and adaptable to the unique movement characteristics of each user. The main ankle movements of the exoskeleton are illustrated in Figure 1.

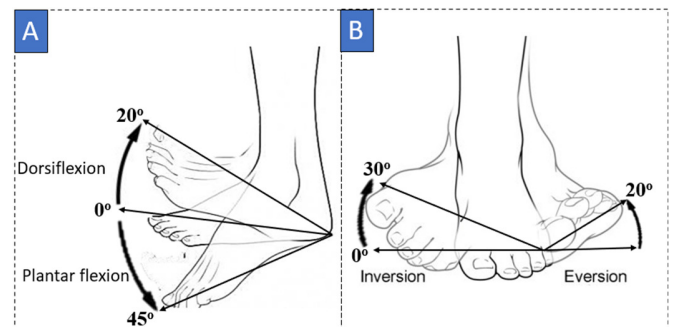


Fig. 1. Primary ankle joint movement mechanisms: (a) dorsiflexion and plantarflexion, (b) inversion and eversion.

The exoskeleton motion planning is adjusted and limited to the natural capacity of the joints to ensure the safety and comfort of the user during operation. The limitations of the exoskeleton range of motion are presented in Table I.

TABLE I. COMPARISON OF THE RANGE OF MOTION BETWEEN ANKLE AND DEVICE

Types of motion	Anatomical range (°)	Proposed device range (°)
Dorsiflexion	20	15
Plantarflexion	45	40
Inversion	30	30
Eversion	20	10

B. Mechanical Structure Design

The mechanical structure of the exoskeleton is designed to support the user in a sitting position, with the lower limbs stabilized so that movement is concentrated only at the ankle joints. This configuration is described in Table II.

TABLE II. MAIN MECHANICAL COMPONENTS OF THE EXOSKELETON

Component	Description
Foot and calf support frame	Maintains the stability and orientation of the lower leg
2-servo motor actuator system	One servo motor controls ankle rotation, the other controls vertical footplate motion
Dual-axis hinge structure	Enables selective dorsiflexion/plantarflexion and inversion–eversion movements
Foot padding and fastening straps	Designed to ensure user comfort and positional accuracy during rehabilitation

The range of motion of the mechanical exoskeleton system is designed based on common physiological values during the rehabilitation process, with the motion angles still limited to prevent injury. Figure 2 illustrates the design concept and structural layout of the exoskeleton.

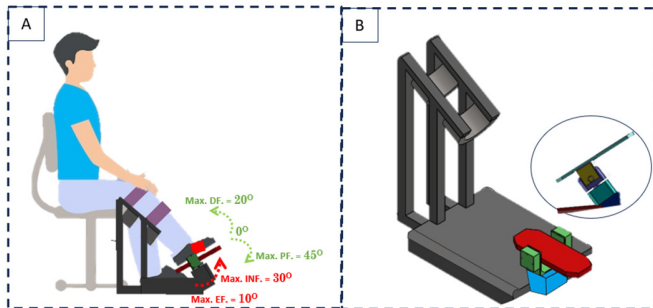


Fig. 2. Exoskeleton design concept and structural layout: (a) actuator placement at the ankle joint, (b) rotational mechanism connected to the joint structure.

C. Motion and Force Analysis

Motion and force analyses were conducted to understand the relationship between kinematic parameters and the actuator torque requirements for supporting the rehabilitation of dorsiflexion–plantarflexion and inversion–eversion movements. The exoskeleton system is designed to mimic the natural movement pattern of the human ankle, taking into account the limitations of a safe and comfortable physiological range of motion for the patient.

D. Exoskeleton Kinematics

The ankle movements are modeled as two independent rotational motions, each representing two DoFs in two primary planes. Inversion and eversion occur along the x-axis, whereas dorsiflexion and plantarflexion take place along the z-axis. For an angular position $\theta(t)$, the velocity $\omega(t)$, and acceleration $\alpha(t)$ are expressed as [20]:

$$\omega(t) = \frac{d\theta(t)}{dt} \tag{1}$$

$$\alpha(t) = \frac{d^2\theta(t)}{dt^2} \tag{2}$$

Two servo actuators are used to control each rotational axis in the exoskeleton design. Ankle movements can be controlled selectively and precisely to accommodate the rehabilitation needs of the patient. Figure 3 provides a visualization of the working space of the 2-DoF ankle exoskeleton. Specifically, Figures 3(a) and 3(b) depict the workspace and the end-effector motion trajectory, respectively. Figure 3(a) shows the exoskeleton's workspace in a two-dimensional plane, with the X-axis representing dorsiflexion–plantarflexion and the Y-axis representing inversion–eversion, forming a pattern of dense and evenly distributed points. Figure 3(b) displays the temporal trajectory of the exoskeleton's end-effector during rehabilitation movement, forming an elliptical pattern due to the simultaneous combination of movements along both axes. This trajectory is generated from harmonic motions with different frequencies for each axis (0.5 Hz for dorsiflexion–

plantarflexion and 0.3 Hz for inversion–eversion), demonstrating the system's ability to produce complex, coordinated movements resembling the natural motion pattern of the ankle. Figure 4 illustrates the performance visualization of the 2-DoF ankle exoskeleton movement.

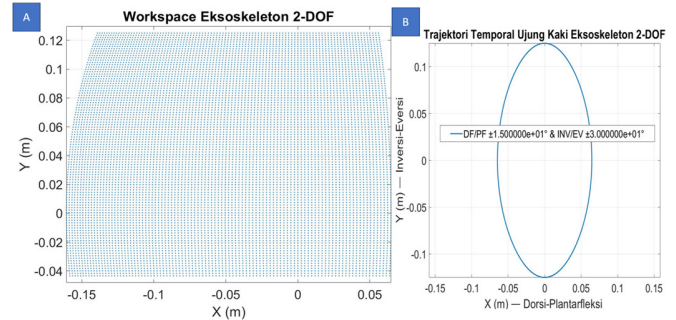


Fig. 3. Visualization of the 2-DoF ankle exoskeleton workspace: (a) 2-DoF exoskeleton workspace, (b) temporal trajectory of the exoskeleton end-effector.

Figures 4(a) and 4(b) show the angular velocity and acceleration profiles of the 2-DoF ankle exoskeleton during rehabilitation movements. The smooth sinusoidal patterns observed along both the dorsiflexion–plantarflexion and inversion–eversion axes indicate rhythmic and coordinated motion. The higher amplitude observed in inversion–eversion reflects the greater movement requirements in the frontal plane. Overall, these graphs demonstrate that the exoskeleton is capable of producing stable, safe movements that align with the natural motion patterns of the ankle.

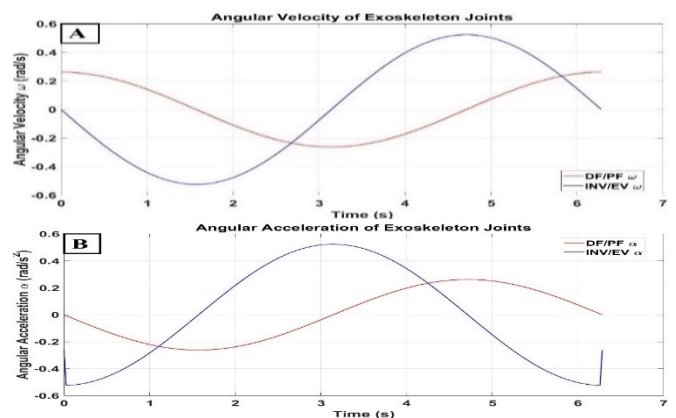


Fig. 4. Performance visualization of the 2-DoF ankle exoskeleton movement: (a) angular velocity of the exoskeleton joint, (b) angular acceleration of the exoskeleton joint.

E. Exoskeleton Dynamics

A dynamic model is used to calculate the torque required by the servo motor for the system to optimally follow the ankle movement trajectory. The calculation of the foot segment weight is based on a body weight of 90 kg, using body mass percentage values from the literature by authors in [19].

TABLE III. CALCULATION OF LEG SEGMENT WEIGHT BASED ON A BODY WEIGHT OF 90 KG

Body segment	Body weight percentage	Calculation	Weight (kg)
Lower leg (knee height)	9.30%	$(90 \text{ kg} \times 9.3\%) / 2$	4.185
Foot sole	2.90%	$(90 \text{ kg} \times 2.9\%) / 2$	1.305
Total weight of one lower limb segment		$(4.185 \text{ kg} + 1.305 \text{ kg})$	5.49

Based on the calculations in Table III, the mass of the foot and sole segment is assumed to be 5.49 kg, based on a body weight of 90 kg [21]. Assuming a segment from the hinge point to the tip of the foot of 0.25 m and modeling the foot as a homogeneous beam, moment of inertia I , force, and total torque $\tau(t)$ on the hinge due to the rotational motion are computed as follows [22]:

$$I = \frac{1}{3}ml^2 \tag{3}$$

$$\tau(t) = I \cdot \alpha(t) + m \cdot g \cdot 2l \cdot \cos(\theta(t)) \tag{4}$$

The calculated values for the moment of inertia, force, and torque are used as the basis for determining the appropriate specifications of the servo motor, ensuring that the exoskeleton can provide optimal support during the rehabilitation process without causing fatigue or injury risks.

Figure 5 shows the torque graph for Joint 1 (dorsiflexion-plantarflexion) and Joint 2 (inversion-eversion) of the ankle exoskeleton over a 10 s period. Assuming a segment mass of 5.49 kg and a length of 0.25 m, the torque for Joint 1 ranges from 12.5 Nm to 13.5 Nm, and for Joint 2, it ranges from 5.5 Nm to 6.8 Nm. The sinusoidal pattern reflects the periodic motion, indicating the need for a powered actuator for Joint 1 and precise control for Joint 2 to support ankle movement rehabilitation.

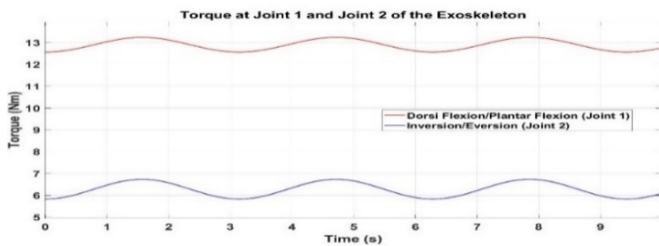


Fig. 5. Visualization of the joint torque in the 2-DoF ankle exoskeleton.

III. EXOSKELETON ROBOT CONTROL SYSTEM

The control system of the exoskeleton robot is designed to regulate the ankle joint movement according to the rehabilitation needs of the user. Figure 6 provides an overview of the control system operation in the exoskeleton. In this system, the input signal (represented by the reference angle θ) is converted into angular velocity (ω) and angular acceleration (α) to calculate the dynamic torque. This torque is then used to determine the amount of force that the actuator must provide to follow the desired trajectory. Each movement is controlled based on a specific angular command directly set through the program. The angular values are explicitly provided in the code

to form the trajectory according to the therapeutic needs. This approach is simple yet effective in ensuring that the rehabilitation movement stays within physiological limits and is safe for the patient. The system can also be equipped with angle sensors (encoders), force or pressure sensors, and microprocessor communication systems such as Arduino or STM32 to implement a real-time closed-loop control. Thus, the exoskeleton can provide responsive, safe, and rehabilitation-specific movement support for the user.

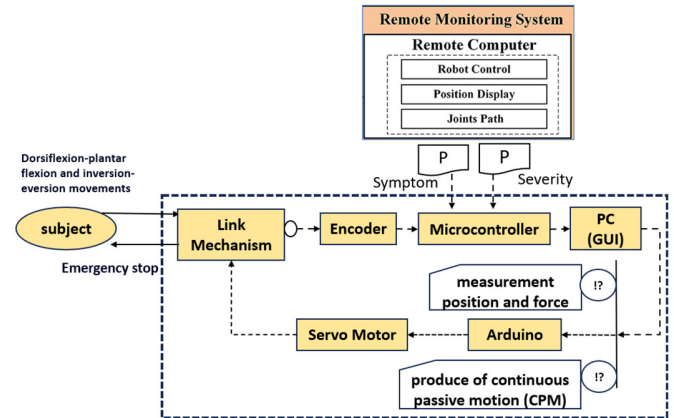


Fig. 6. Overview of the control system operation in the exoskeleton.

IV. EXPERIMENTAL SETUP AND RESULTS

The ankle exoskeleton is designed to be applied directly to the human ankle, making safety, stability, and reliability the primary focus. Testing is performed to evaluate the actuator's response to the programmed movement angles and the accuracy of the motion trajectory tracking. This evaluation aims to ensure the system's performance before it is further applied in a rehabilitation context.

A. Robot Motion Response Experiment

The first evaluation was conducted to demonstrate the system's ability to reach the target angle with a response time of 10 movement direction changes.

Figure 7 shows that the exoskeleton is able to follow the target angle with a smooth and stable response pattern, despite a time delay and gradual increase toward the final angle. Plantar flexion and inversion exhibit a faster response compared to dorsiflexion and eversion, indicating that the exoskeleton's control system has been designed to avoid sudden movements and maintain motion stability, which is crucial for rehabilitation applications.

B. Robot Trajectory Tracking Experiment

Trajectory tracking experiments were conducted to evaluate the ability of the exoskeleton system to precisely follow the specified joint angles at the ankle. Each movement was compared between the input angle trajectory and the actual tracking trajectory. Testing was conducted to determine the degree of alignment between the target angle and the actual angle achieved by the motor actuator. The results from this experiment are presented in Figure 8.

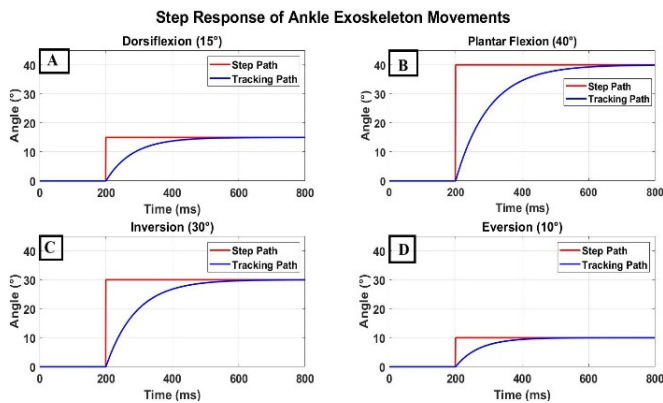


Fig. 7. Angular response of the ankle joint to target movements: (a) 15°, (b) 40°, (c) 30°, (d) 10°.

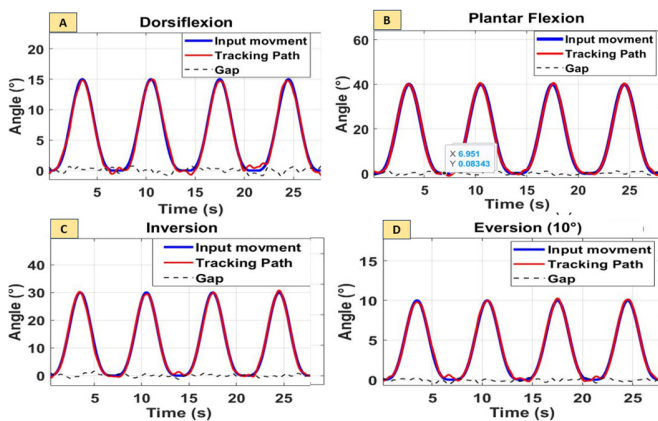


Fig. 8. Trajectory tracking performance of the ankle exoskeleton at angular velocity $\omega=0.897$ rad/s.

Figure 8 demonstrates the exoskeleton's excellent tracking capability, with each movement cycle taking 28 s, resulting in a movement period (T) of approximately 7 s and an angular velocity (ω) of 0.897 rad/s. The error value between the input movement path and the tracking path indicates that the system performs well. The average error (gap) across the four types of movements is approximately $\pm 0.15^\circ$, reflecting the system's high accuracy and precision in following the desired movement trajectory.

C. Human-Machine Usability Testing

The reliability, stability, and safety of the ankle rehabilitation exoskeleton system were evaluated through trajectory tracking tests, as illustrated in Figure 9. The test assessed the system's ability to follow physiological angle commands during dorsiflexion, plantarflexion, inversion, and eversion movements. The test focused on how the actuator responds to physiological profile-based input signals. In addition, the characteristics of seven healthy individuals with varying body weight ranges were considered to assess the adaptation of the exoskeleton to different user conditions. This protocol has been approved by the Health Research Ethics Committee of Dr. Moewardi Hospital, Surakarta (No. 1.439/V/HREC/2024), and is in accordance with the principles of the Declaration of Helsinki, emphasizing voluntary participation, informed consent, subject safety, and

confidentiality during the study. All participants were explained the purpose, benefits, and potential risks, and they provided written consent before participating. The exoskeleton is equipped with an emergency button feature to ensure the comfort and safety of the subjects during the test.



Fig. 9. Experimental setup showing a healthy subject wearing the ankle rehabilitation exoskeleton during testing.

Figure 10 shows the angular tracking results for each participant. The results showed that the exoskeleton system was able to consistently track physiological angles in all types of movements with almost identical curve patterns in the body weight range of 60–80 kg. The angle curves showed good stability and cycle repetition without significant deviations between individuals, indicating that variations in body weight did not significantly affect actuator performance. The average angle tracking error values for each movement were 0.82° for dorsiflexion, 1.03° for plantarflexion, 0.76° inversion, and 1.21° for eversion. There was a slight fluctuation in the peak of the eversion curve, but the error value was still within the tolerance limit of the system.

A statistical analysis was performed on the angle tracking error data from each participant performing the four main types of movements: dorsiflexion, plantarflexion, inversion, and eversion. The results are shown in Table IV.

TABLE IV. DESCRIPTIVE STATISTICS OF EXOSKELETON ANGLE TRACKING ERROR

Movement	μ ($^\circ$)	σ ($^\circ$)	σ^2	Min ($^\circ$)	Max ($^\circ$)
Dorsiflexion	0.82	0.0216	0.00047	0.79	0.85
Plantarflexion	1.03	0.0216	0.00047	1	1.06
Inversion	0.75	0.0151	0.00023	0.74	0.78
Eversion	1.21	0.0216	0.00047	1.18	1.24

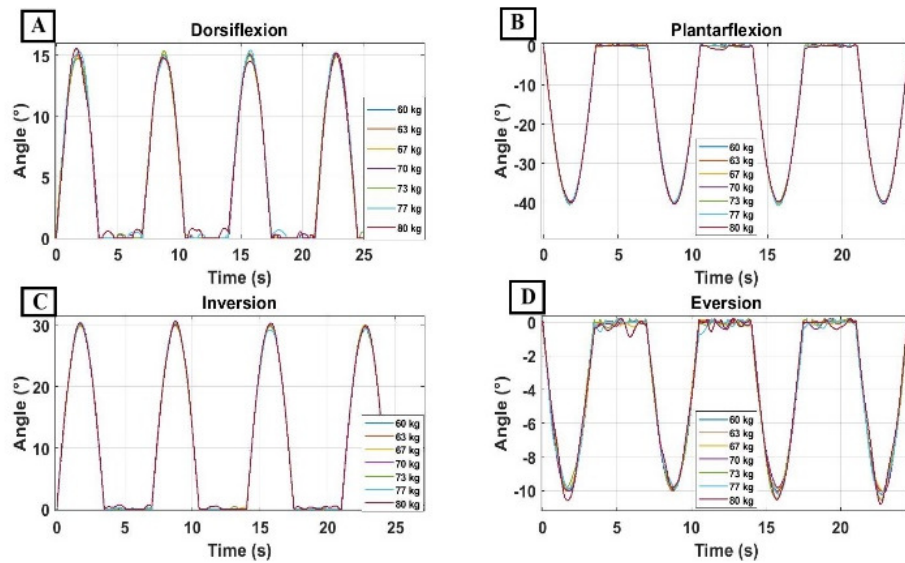


Fig. 10. Joint-angle tracking response for users with body weights of 60–80 kg.

As shown in Table IV, the average error for the four movements was between 0.75° and 1.21° , with a low standard deviation of between 0.0151° and 0.0216° . The narrow range of error values between individuals (0.03° – 0.06°) indicates the system's consistency and stable tracking performance. The statistical tests revealed that the exoskeleton system exhibited consistent and stable tracking performance with minimal inter-individual deviation. These results support the use of the system for ankle motion rehabilitation in post-stroke patients.

V. CONCLUSION

This study successfully developed a Two-Degree-of-Freedom (2-DoF) ankle exoskeleton to support dorsiflexion–plantarflexion and inversion–eversion rehabilitation in post-stroke patients. Initial validation through kinematic simulation demonstrated a maximum angular error of only 0.65° compared to the target trajectory, which ranged from $+10^\circ$ to -20° for dorsiflexion–plantarflexion and $\pm 10^\circ$ for inversion–eversion. In addition, dynamics simulations of the 2-DoF ankle exoskeleton, using a force and mass model of the subject's foot segment, revealed that the maximum required torque to drive the system was approximately 1.05 Nm for dorsiflexion–plantarflexion and 0.65 Nm for inversion–eversion. The kinematic and dynamic simulation results remained within the working capacity of the servo motor, ensuring the system's safety for real human load application.

Experimental testing of the 2-DoF exoskeleton prototype was conducted on several subjects with body weights ranging from 60 kg to 80 kg. The results showed an average angular error of $\pm 1.9^\circ$ without load and $\pm 2.7^\circ$ with load during dorsiflexion–plantarflexion movements. Overall, the system demonstrated consistent stability, accuracy, and performance in following the programmed motion trajectory. This is in contrast to the 2-DoF ankle exoskeleton design developed by authors in [11], which uses a Pneumatic Artificial Muscle (PAM)-based system that requires an external air supply and complex nonlinear control. This study's exoskeleton system design is

able to achieve similar motion accuracy without additional infrastructure. Furthermore, unlike the bidirectional cable tendon actuation system proposed by authors in [12], which utilizes adaptive neural network PID-based control to overcome cable length variation and system uncertainty, the approach in this study uses a simple servo motor mechanism with preset input angle control. This study's exoskeleton design offers the advantages of simplicity, ease of use, and potential for application in homes and rehabilitation facilities with limited resources. Therefore, it presents a safe, effective, and practical rehabilitation solution for post-stroke patients.

REFERENCES

- [1] X. Zhang, Z. Yue, and J. Wang, "Robotics in Lower-Limb Rehabilitation after Stroke," *Behavioural Neurology*, vol. 2017, no. 1, June 2017, Art. no. 3731802, <https://doi.org/10.1155/2017/3731802>.
- [2] K. I. Paraskevas, "Prevention and treatment of strokes associated with carotid artery stenosis: a research priority," *Annals of Translational Medicine*, vol. 8, no. 19, pp. 1260–1260, Oct. 2020, <https://doi.org/10.21037/atm-2020-cass-25>.
- [3] M. da Miao, X. shan Gao, J. Zhao, and P. Zhao, "Rehabilitation robot following motion control algorithm based on human behavior intention," *Applied Intelligence*, vol. 53, no. 6, pp. 6324–6343, Mar. 2023, <https://doi.org/10.1007/s10489-022-03823-7>.
- [4] K. Bamforth, P. Rae, J. Maben, H. Lloyd, and S. Pearce, "Perceptions of healthcare professionals' psychological wellbeing at work and the link to patients' experiences of care: A scoping review," *International Journal of Nursing Studies Advances*, vol. 5, Dec. 2023, Art. no. 100148, <https://doi.org/10.1016/j.ijnsa.2023.100148>.
- [5] C. J. Winstein *et al.*, "Guidelines for Adult Stroke Rehabilitation and Recovery," *Stroke*, vol. 47, no. 6, pp. e98–e169, June 2016, <https://doi.org/10.1161/STR.0000000000000098>.
- [6] D. M. G. Preethichandra *et al.*, "Passive and Active Exoskeleton Solutions: Sensors, Actuators, Applications, and Recent Trends," *Sensors*, vol. 24, no. 21, Nov. 2024, Art. no. 7095, <https://doi.org/10.3390/s24217095>.
- [7] R. K. Saleh, W. S. Aboud, and S. M. Haris, "A Review Study for Robotic Exoskeletons Rehabilitation Devices," *Al-Nahrain Journal for Engineering Sciences*, vol. 26, no. 6, pp. 63–73, July 2023.
- [8] S. Z. Ying, N. K. Al-Shammari, A. A. Faudzi, and Y. Sabzehmeidani, "Continuous Progressive Actuator Robot for Hand Rehabilitation,"

- Engineering, Technology & Applied Science Research*, vol. 10, no. 1, pp. 5276–5280, Feb. 2020, <https://doi.org/10.48084/etasr.3212>.
- [9] Y. Xing and C. Lv, "Dynamic State Estimation for the Advanced Brake System of Electric Vehicles by Using Deep Recurrent Neural Networks," *IEEE Transactions on Industrial Electronics*, vol. 67, no. 11, pp. 9536–9547, Nov. 2020, <https://doi.org/10.1109/TIE.2019.2952807>.
- [10] L. Huang, J. Zheng, Y. Gao, Q. Song, and Y. Liu, "A Lower Limb Exoskeleton Adaptive Control Method Based on Model-free Reinforcement Learning and Improved Dynamic Movement Primitives," *Journal of Intelligent & Robotic Systems*, vol. 111, no. 1, Feb. 2025, Art. no. 24, <https://doi.org/10.1007/s10846-025-02230-7>.
- [11] X. Zhang, H. Li, Z. Lu, and G. Yin, "Homology Characteristics of EEG and EMG for Lower Limb Voluntary Movement Intention," *Frontiers in Neurobotics*, vol. 15, June 2021, Art. no. 642607, <https://doi.org/10.3389/fnbot.2021.642607>.
- [12] S. Hassani and U. Dackermann, "A Systematic Review of Advanced Sensor Technologies for Non-Destructive Testing and Structural Health Monitoring," *Sensors*, vol. 23, no. 4, Feb. 2023, Art. no. 2204, <https://doi.org/10.3390/s23042204>.
- [13] Z. Chen, Q. Guo, H. Xiong, D. Jiang, and Y. Yan, "Control and Implementation of 2-DOF Lower Limb Exoskeleton Experimentation Platform," *Chinese Journal of Mechanical Engineering*, vol. 34, no. 1, Feb. 2021, Art. no. 22, <https://doi.org/10.1186/s10033-021-00537-8>.
- [14] S. Kim and S. Kwon, "Robust transition control of underactuated two-wheeled self-balancing vehicle with semi-online dynamic trajectory planning," *Mechatronics*, vol. 68, June 2020, Art. no. 102366, <https://doi.org/10.1016/j.mechatronics.2020.102366>.
- [15] D. P. Losey and M. K. O'Malley, "Trajectory Deformations From Physical Human–Robot Interaction," *IEEE Transactions on Robotics*, vol. 34, no. 1, pp. 126–138, Feb. 2018, <https://doi.org/10.1109/TRO.2017.2765335>.
- [16] C. L. Brockett and G. J. Chapman, "Biomechanics of the ankle," *Orthopaedics and Trauma*, vol. 30, no. 3, pp. 232–238, June 2016, <https://doi.org/10.1016/j.mporth.2016.04.015>.
- [17] R. Baud, A. R. Manzoori, A. Ijspeert, and M. Bouri, "Review of control strategies for lower-limb exoskeletons to assist gait," *Journal of NeuroEngineering and Rehabilitation*, vol. 18, no. 1, July 2021, Art. no. 119, <https://doi.org/10.1186/s12984-021-00906-3>.
- [18] S. Ibaraki and R. Saito, "Novel kinematic model of articulated arm coordinate measuring machine with angular position measurement errors of rotary axes," *CIRP Annals*, vol. 72, no. 1, pp. 449–452, Jan. 2023, <https://doi.org/10.1016/j.cirp.2023.03.035>.
- [19] S. Bruno, M. José, S. Filomena, C. Vítor, M. Demétrio, and B. Karolina, "The Conceptual Design of a Mechatronic System to Handle Bedridden Elderly Individuals," *Sensors*, vol. 16, no. 5, May 2016, Art. no. 725, <https://doi.org/10.3390/s16050725>.
- [20] E. W. Abryandoko, S. Susmartini, P. W. Laksono, and L. Herdiman, "Simulation and Modeling of Hybrid Assistive Robotic Neuromuscular Dynamic Stimulation for Upper Limb Rehabilitation," *Journal of Applied Science and Engineering*, vol. 28, no. 5, pp. 925–933, July 2024, [https://doi.org/10.6180/jase.202505_28\(5\).0002](https://doi.org/10.6180/jase.202505_28(5).0002).
- [21] H. S. Choi, C. H. Lee, and Y. S. Baek, "Design and Validation of a Two-Degree-of-Freedom Powered Ankle-Foot Orthosis with Two Pneumatic Artificial Muscles," *Mechatronics*, vol. 72, Dec. 2020, Art. no. 102469, <https://doi.org/10.1016/j.mechatronics.2020.102469>.
- [22] T. Lee, I. Kim, and Y. S. Baek, "Design of a 2DoF Ankle Exoskeleton with a Polycentric Structure and a Bi-Directional Tendon-Driven Actuator Controlled Using a PID Neural Network," *Actuators*, vol. 10, no. 1, Jan. 2021, Art. no. 9, <https://doi.org/10.3390/act10010009>.